

## Transportation of a Low-voltage Sheet Helical Electron Beam for Confocal Gyrotron with Pulsed Magnetic System

Yu.S. Kovshov<sup>1</sup>, S.V. Starokozhev<sup>1</sup>, S.A. Kishko<sup>1</sup>, S.S. Ponomarenko<sup>1</sup>, S.A. Vlasenko<sup>1,2</sup>,  
A.N. Kuleshov<sup>1</sup>, **B.P. Yefimov<sup>1</sup>**

<sup>1</sup> *O.Ya. Usikov Institute for Radiophysics and Electronics, National Academy of Sciences of Ukraine, 12, Ac. Proscura Str., 61085 Kharkiv, Ukraine*

<sup>2</sup> *V.N. Karazin Kharkiv National University, 4, Svobody Sq., 61022 Kharkiv, Ukraine*

(Received 05 May 2015; published online 20 October 2015)

Gyrotrons with opened cavities which consist of two confocal cylindrical mirrors are promising sources of electromagnetic radiation in submillimeter range because of a sufficient level of output power, frequency stability and the possibility of tuning the operating frequency over a wide range. It is necessary for a large number of scientific and practical applications. In this paper, for effective excitation of oscillations of the electrodynamic system of a confocal CRM-gyrotron in 4-millimeter wavelength range we propose to use a sheet helical electron beam formed by the planar magnetron injection gun in an adiabatically increasing magnetic field of the order of 3 T in the cavity region. In the paper we offer the pulsed magnetic system which creates a magnetic field with a high degree of uniformity in the cavity region and the field with optimal distribution for adiabatic input of electron beam. The possibility of forming a helical sheet of an electron beam with a high value of the pitch-factor and low-velocity and electron energy spread was shown as a result of the trajectory analysis.

**Keywords:** Low-voltage cyclotron resonance maser, Sheet helical electron beam, Pulsed magnetic system, Planar magnetron-injection gun, Confocal gyrotron.

PACS number: 41.85.Ja

### 1. INTRODUCTION

Currently, electromagnetic radiation emitters in the millimeter and submillimeter wavelength ranges are widely in demand in various scientific and practical applications. Nuclear magnetic resonance (NMR) spectroscopy using dynamic polarization of nuclei is one of such applications, and electromagnetic radiation sources are necessary to directly increase the sensitivity during the spectral analysis. However, absorption spectra of the studied substances can be in different frequency ranges and, as a result, the requirements of tuning the operating frequency in a wide frequency band are advanced to electromagnetic radiation sources. In addition, the possibility of frequency adjustment for sub-THz gyrotrons is necessary [1, 2]. Moreover, power level of the electromagnetic radiation source should be sufficient for the effective amplification of NMR.

Electron-vacuum electromagnetic radiation sources are currently used in submillimeter spectroscopy. Backward-wave tubes (BWT) have a sufficiently wide operating frequency tuning; however, their output power in the millimeter and submillimeter wavelength ranges is very small that limits their use in spectroscopy. On the other hand, there are CRM (cyclotron-resonance masers) gyrotrons, which in these frequency ranges have high output power. However, due to a comparatively high  $Q$ -factor of their electrodynamic systems, frequency tuning there is only possible within narrow limits that makes it very difficult to adjust frequency for the studied sample and complicates their use in this field of research. In connection with the above-listed, there are two ways to solve this problem. The first way is the increase in the output power of BWT [3], and the second one – is the increase in the operating frequency tuning in the CRM-gyrotrons [1, 2].

Increase in the gyrotron operating frequency tuning is possible due to the use of electrodynamic systems with variable geometric dimensions, as it is shown in [4, 5]. In particular, it was proposed in [5] to use gyrotron with the cavity composed of two cylindrical mirrors, where it is possible to tune the natural frequency of the device cavity on account of the change in the distance between mirrors. To improve the efficiency of similar gyrotrons, it was offered in [6] to use a sheet helical electron beam (HEB) with high electron rotational energy as an active medium; and electron-optical system for the formation of the same beam was calculated in [7]. The numerical simulation results of the interaction of a sheet HEB with a high-frequency field of confocal cavity have shown the possibility of an effective excitation of oscillations [8].

The desired parameters of HEB are achieved in the magnetic system; and an important role is played not only by the field value in the cavity region, but also by the distribution of a magnetic field along the whole beam pass. For gyrotrons in 4-millimeter wavelength range it is necessary to provide the magnetic field of the order of 2.7 T. The use of “warm” solenoids for the creation of such high magnetic fields is complicated due to severe overheating of the magnetic system. In this connection, superconducting magnetic systems [9] or pulsed ones [10] are used. In this work, for the formation and transportation of a sheet HEB we have calculated the pulsed magnetic system, which forms a magnetic field up to 3 T in the maximum and has compact dimensions.

In the present work, Section 1 gives estimation of the parameters of a sheet HEB, such as the transverse beam dimensions, electron velocity and energy spreads in the beam, for the effective interaction with a high-frequency field of a confocal gyrotron.

Section 2 offers results on the development, calcula-

tion and optimization of the pulsed magnetic system for a confocal gyrotron in 4-millimeter wavelength range.

Section 3 presents the numerical simulation results on the focusing and transportation of a sheet HEB in the field of the developed pulsed magnetic system and the trajectory analysis results for the formed electron beam.

## 2. THE REQUIREMENTS TO A SHEET HEB OF A CONFOCAL GYROTRON

Electrodynamic system of a confocal gyrotron represents two cylindrical mirrors with annular inserts at the edges. Calculation of the confocal cavity is performed in [8], where it is shown that for the effective excitation of oscillations of such a cavity, electron beam should completely hit the spot of a high-frequency field of the oscillation excited in the cavity. Confocal cavity was designed to operate in 4-millimeter wavelength range on the  $H_{03}$ -mode. The cavity has the following dimensions: length 26.25 mm, mirror width 10 mm, distance between the mirrors 6 mm. In this cavity, based on [11], the maximum width of the field spot of the oscillation excited in the cavity will be equal to the mirror half-width that in this case is about 5 mm. Thus, the optimal beam width should be of the order of 5 mm and the beam thickness should be no larger than the operating half wavelength that in the case of 4-millimeter range is equal to 2 mm. Since in a confocal gyrotron the natural frequency of the cavity will vary with changing distance between the mirrors, then the beam thickness should be of the order of 1 mm in order to hit the spot maximum of the electric field strength and effectively interact with a high-frequency cavity field.

Besides the geometric dimensions of the electron beam, for the implementation of the effective interaction with a high-frequency field of the confocal cavity, the beam should have a sufficient electron rotational energy (pitch-factor is more than 1) and the minimum electron velocity and energy spreads in the beam.

The electron efficiency of a gyrotron in the presence of the electron velocity spread can be calculated using the following expression [12]:

$$\eta_{el} = \int_0^\pi v_{\parallel} f(v_{\perp})(v_{\perp}/v)^2 \left[ 1 - \frac{1}{2\pi} \int_0^{2\pi} w(\mu, v_0') dv_0' \right] dv_{\perp}.$$

Here  $f(v_{\perp})$  is the rotational velocity distribution function of electrons;  $v_0'$  is the initial phase of the electron motion;  $v$  is the total electron velocity;  $v_{\parallel}$  is the translational component of the electron velocity;  $v_{\perp}$  is the rotational component of the electron velocity;  $w$  is the relative rotational energy of an electron (is determined by the numerical solution of the field equations and equations of electron motion with different velocities);  $\mu$  is the non-isochronous parameter. Based on the results of the calculations performed in [12], with increasing spread of electron rotational velocities there is decrease in the optimal value of the pitch-factor and increase in the optimal interaction space length that reduces the electron efficiency of a gyrotron. The maximum electron efficiency of a gyrotron (of the order of 60 %) can be achieved for the value of the spread of electron rotational velocities not exceeding 8 %. Thus, spread of electron rotational velocities in the formed beam should not exceed 8 %.

As shown in [13], because of the relativistic dependence of the gyrofrequency on the energy, the efficiency of gyrotrons is sensitive to even a slight spread of electron initial energies. To minimize this effect, the minimum energy spread will be determined by the following expression [13]:

$$\frac{\Delta E}{E} \ll \frac{1}{N}.$$

Here  $N$  is the number of cyclotron rotations on the interaction length,  $E$  is the electron energy. Thus, the electron energy spread for a confocal gyrotron of 4-millimeter wavelength range with the interaction space length of the order of 26 mm should not exceed 2 %.

In order to carry out the trajectory analysis and determine the energy characteristics of a sheet HEB, the solution of the equations of electron motion in electric and magnetic fields is necessary. However, in contrast to tubular axially-symmetrical HEB utilized in classical gyrotrons, analytical formulas for a sheet HEB become unusable because of the absence of axial symmetry and, as a consequence, a complex notation of the Bush theorem in the orthogonal system of coordinates. Thus, the methods of direct numerical simulation were used to perform the trajectory analysis of a sheet HEB in a magnetic field of the pulsed magnetic system.

## 3. COMPACT PULSED MAGNETIC SYSTEM

In gyrotrons, wavelength of generated electromagnetic oscillations directly depends on the cyclotron electron rotation frequency in the beam, and, as a result, on the value of the magnetic field in the interaction space and can be estimated by the formula  $\lambda = 10.7/B$  [13], where  $\lambda$  is the wavelength in mm and  $B$  in the magnetic field induction in T. Thus, magnetic induction should be of the order of 2.7 T to operate in 4-millimeter wavelength range. Since in gyrotrons the cyclotron resonance band is about several percent, then in order to preserve optimal operating mode of the device, it is necessary during the generation process to maintain the magnetic field value within tenths of a percent of the optimal one [10]. To fulfill this requirement, current pulse duration in the solenoid should exceed several times the generation duration and have the region with almost constant current over a period of device generation.

To generate a pulsed magnetic field, the scheme [14] illustrated in Fig. 1 was used, in which magnetic field is created by the pulsed discharge current of reservoir capacitors  $C$  through the coil of a solenoid without a core with inductance  $L$  and small active resistance  $R$ . As a key initiating the discharge process, thyatron  $T$  was used. In order to prevent a negative charge of the capacitor, the discharging circuit consisted of the diode  $D$  and resistor  $R_1$  limiting the discharge current was utilized.

When the thyatron key  $T$  is opened, the current in the circuit will vary according to the following law [14]:

$$I = \frac{U_0}{Z} \frac{\omega_0}{\omega} e^{-\delta t} \sin \omega t,$$

where

$$\omega_0^2 = 1/LC, \omega^2 = \omega_0^2 - \delta^2, \\ \omega = 2\pi/T, \delta = R/2L,$$

$Z = \sqrt{L/C}$  is the circuit impedance. Based on these expressions, parameters of a pulsed solenoid were calculated. A rectangular copper bus of the section of  $4 \cdot 1.5 \text{ mm}^2$  was used for winding. The inner solenoid radius is equal to 20 mm, length – 120 mm, a number of loops – 800. For these parameters, the outer solenoid radius is 60 mm and inductance – 8.4 mH. The time dependence of the capacitor discharge current with capacity of  $1000 \mu\text{F}$  at the voltage of 1600 V through the solenoid is illustrated in Fig. 2.

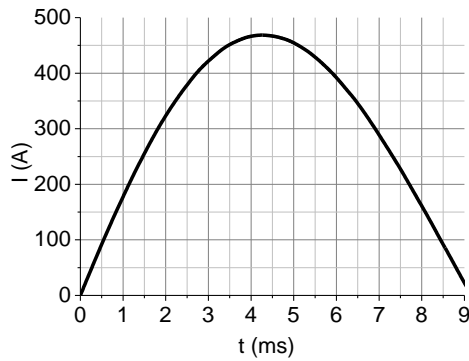


**Fig. 2** – Dependence of the capacitor discharge current through the solenoid versus the time

Estimated value of the magnetic field can be determined by the following formula:

$$B_0 = \mu_0 n I_0 \cos \frac{D}{l}.$$

Here,  $B_0$  is the magnetic induction,  $\mu_0$  is the vacuum permeability,  $n$  is the number of loops,  $I_0$  is the current through the solenoid,  $D$  is the solenoid diameter,  $l$  is the solenoid length. However, magnetic field value obtained using this formula will be larger than the experimental one that is caused by high magnetic field losses on the loops of greater diameter. In connection with this, a more precise calculation of the magnetic field value as well as its distribution were performed using the computer simulation methods.

The given magnetic system allows to obtain magnetic field of the value of about 2.9 T at the solenoid current of 450 A. As seen from Fig. 2, the current pulse duration is approximately equal to 9 ms, at that, pulse duration, within which the change in the magnetic field value does not exceed 0.25 %, makes 280  $\mu\text{s}$ .

To increase the degree of homogeneity of the magnetic field distribution in the interaction space, optimization of the pulsed magnetic system design was implemented. Instead of a single unitary 120 mm solenoid, two 60 mm solenoids were used that together with the change in the distance between them allowed to achieve a high degree of homogeneity in the distribution of the magnetic field longitudinal component in the interaction space. Design of the magnetic system and distribution of the magnetic field longitudinal component in the region of a uniform magnetic field depending on the distance between solenoids is shown in Fig. 3 and Fig. 4, respectively.

As seen from Fig. 4, 4 mm is the optimal distance between solenoids of the magnetic system, at which heterogeneity in the distribution of the magnetic field longitudinal component in 40 mm region does not exceed 1 %.

To increase the degree of homogeneity of the magnetic field longitudinal component in the emitter area, a correcting solenoid in the region of magnetron-injector gun (MIG) was utilized. However, the use of the correcting solenoid in the MIG region leads to heterogeneity in the magnetic field distribution in the interaction space. To eliminate this heterogeneity, the second correcting solenoid located at the same distance on the other side of the magnetic systems was applied. Design of the magnetic system with two correcting solenoids is given in Fig. 5.

Distribution of the magnetic field longitudinal component in the emitter area without the use of a correcting solenoid and with its application is shown in Fig. 6.

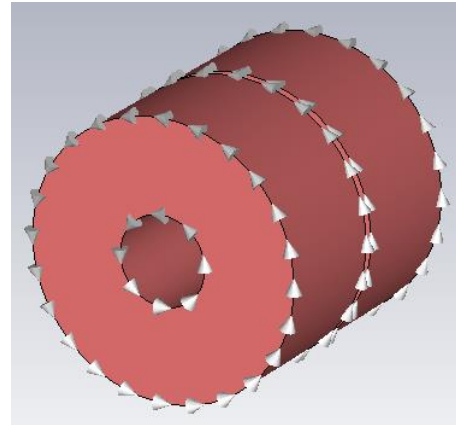


**Fig. 3** – Design of the pulsed magnetic system

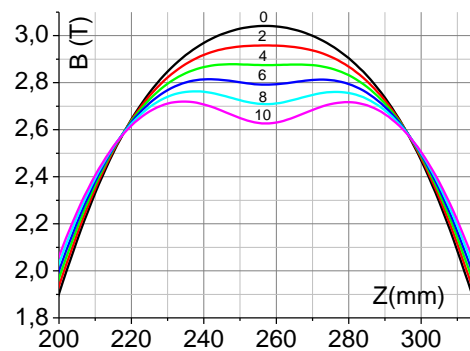


**Fig. 4** – Distribution of the magnetic field longitudinal component in the region of a uniform magnetic field

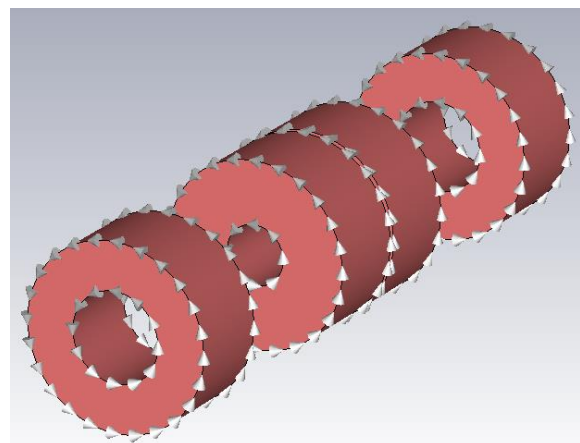


**Fig. 5** – Design of the pulsed magnetic system with two correcting solenoids

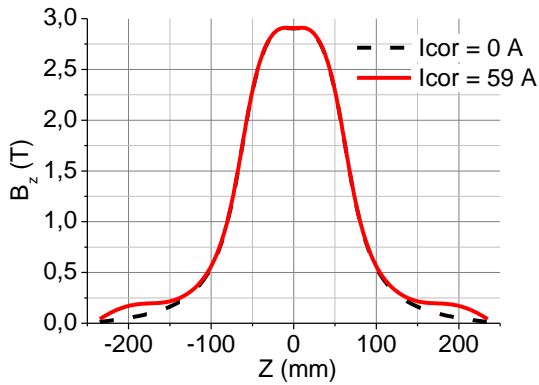


Fig. 6 – Distribution of the magnetic field longitudinal component along the system axis

As seen from Fig. 6, the use of a correcting solenoid in the MIG emitter area allows to increase homogeneity of the magnetic field distribution in the region of electron beam formation in both the longitudinal and transverse directions (see Fig. 7). Emitter boundaries are shown in Fig. 7 by vertical black lines.

As seen from Fig. 7, the use of a correcting solenoid decreases heterogeneity in the magnetic field distribution in the emitter area from 0.9 % to 0.3 %. An increasing magnetic field behavior on the emitter edges stemming from the use of a correcting solenoid allows to decrease the rotational energy of extreme electrons of the beam and, thus, compensate the action of space charge forces in the beam.

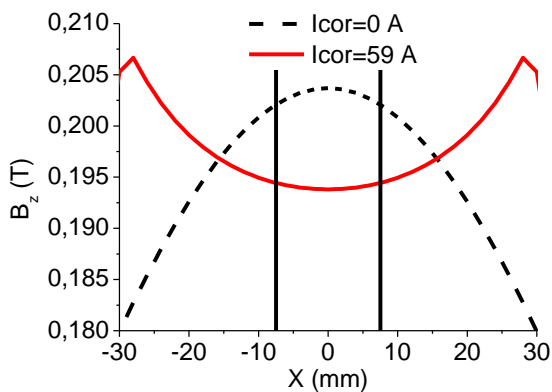


Fig. 7 – Distribution of the magnetic field longitudinal component in the cross-section in the emitter area

#### 4. FORMATION AND TRANSPORTATION OF A SHEET HEB IN THE FIELD OF THE CALCULATED PULSED MAGNETIC SYSTEM

MIG design described in [7, 8] was used for the formation of a sheet low-voltage HEB. This MIG is rated at the value of accelerating voltage up to 6 kV at the maximum beam current of 300 mA. In the operating mode, to achieve the optimal beam parameters, magnetic induction in the MIG area should be approximately equal to 0.2 T. Based on this requirement, the position of a planar MIG in the magnetic field formed by the calculated pulsed magnetic system was selected.

Trajectory analysis of sheet HEB was performed by the numerical simulation methods using magnetic systems without and with a correcting solenoid. The obtained dependences of the spread of the electron velocity compo-

nents, electron energies, and values of the pitch-factor on the magnetic field value in the emitter area are represented in Fig. 8a, b.

As seen from Fig. 8a, b, the use of a correcting solenoid allows to achieve larger pitch-factor of the order of 1.7 in the absence of reflected electrons, while without a correcting solenoid at the pitch-factor of 1.5 reflected electrons already appear. It is also seen from Fig. 8a, b that at such high values of the pitch-factor (1.5-1.7) the obtained electron velocity spreads do not exceed 10 % for the longitudinal velocity component and 5 % for the rotational one, electron energy spread does not exceed 1.5 % that indicates the possibility of the effective use of the obtained sheet HEB in a confocal gyrotron.

Profiles of the sheet HEB cross-section with and without the use of a correcting solenoid are shown in Fig. 9. By comparison, the profiles are obtained at the same value of the beam pitch-factor of the order of 1.3.

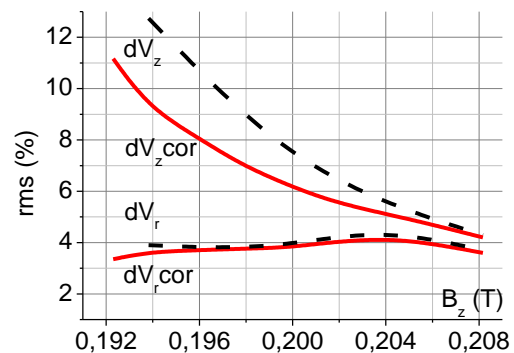


Fig. 8a – Dependence of the spread of the electron velocity component on the magnetic field value

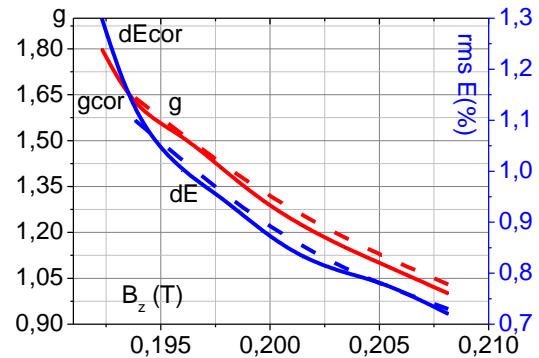


Fig. 8b – Dependence of the electron energy spread and pitch-factor on the magnetic field value

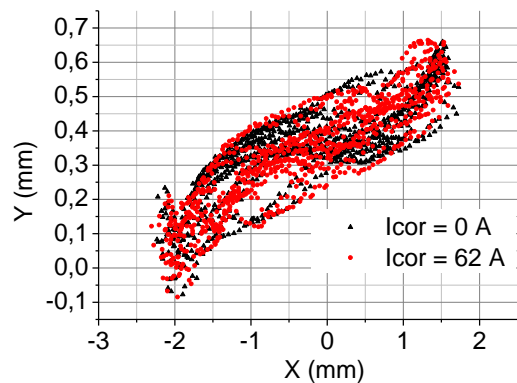


Fig. 9 – Profiles of the beam cross-sections in the area of a uniform magnetic field

It is seen from Fig. 9 that both beams have a strip profile of the cross-section with minimal distortions.

Configuration of a sheet HEB is shown in Fig. 10.

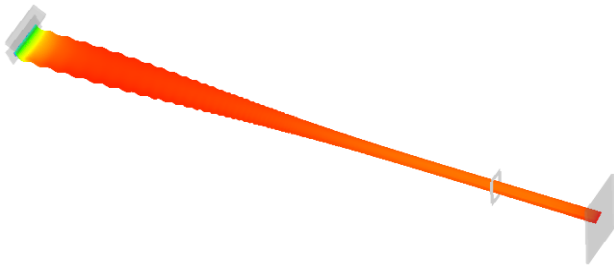


Fig. 10 – Configuration of a sheet HEB

The results of the performed calculations on the formation and transportation of a sheet HEB indicate the applicability of the calculated pulsed magnetic system for the formation of a beam with the required parameters. As seen from the results of the trajectory analysis, the use of correcting solenoids will allow to increase the value of the beam pitch-factor in the absence of reflected electrons and also facilitate correction of the beam parameters and provide protection of the gun emitter from the secondary electron bombardment in the case of synchronization violation between high voltage pulses and solenoid current pulses. It also follows from the calculations that in the absence of correcting solenoids the formed sheet HEB will have energy characteristics which will allow its effective use in a confocal gyrotron, but with a lower pitch-factor of the beam. This is caused by sufficiently small lateral dimensions of the emitter of about 15 mm resulting in the fact that the magnetic field change in

the transverse direction of the emitter does not exceed 1 % without the use of a correcting solenoid. However, with increasing emitter length, the use of correcting solenoids becomes necessary as it is shown in [15].

## 5. CONCLUSIONS

The pulsed magnetic system for the formation of a magnetic field up to 3 T in 40 mm gap has been calculated in this work. To increase the degree of homogeneity of the distribution of the magnetic field longitudinal component in the interaction space, an indent, whose value during the performed optimization was about 4 mm, was added at a section of 40 mm length between solenoids of the magnetic systems. To decrease the spreads of the electron velocity components and electron energies in the beam at the maximum achievable value of the beam pitch-factor, a supplementary correcting solenoid in the MIG emitter area was calculated. The use of the calculated correcting solenoid allows to increase the pitch-factor from 1.5 to 1.7 in the absence of reflected electrons that will enhance the electron efficiency of the device. The results of the performed trajectory analysis have shown that the formed sheet HEB has minimal distortions in the profile in the interaction space and energy characteristics acceptable for its effective use in a confocal gyrotron.

## ACKNOWLEDGEMENTS

The authors of this paper express their gratitude to M.Yu. Glyavin (Institute of Applied Physics of Russian Academy of Sciences, Nizhny Novgorod) for assistance in performing the calculations and discussing the results.

## REFERENCES

- O. Dumbrajs, T. Idehara, *J. Infrared Milli Terahz Waves* **31** No 11, 1265 (2010).
- A.C. Torrezan, Seong-Tae Han, I. Mastovsky, M.A. Shapiro, J.R. Sirigiri, R.J. Temkin, A.B. Barnes, R.G. Griffin, *IEEE Trans. Plasma Sci.* **38** No 6, 1150 (2010).
- E.M. Khutoryan, S.S. Ponomarenko, S.A. Kishko, K.A. Lukin, A.N. Kuleshov, B.P. Yefimov, *Izv. VUZov. Prikladnaya nelineynaya dinamika* **21** No 2, 9 (2013).
- I.I. Antakov, S.N. Vlasov, V.A. Gintsburg, L.I. Zagryadskaya, L.V. Nikolayev, *Elektronnaya tekhnika: Elektronika SVCh* **1** No 8, 20 (1975).
- Wen Hu, M.A. Shapiro, K.E. Kreicher, R.J. Temkin, *IEEE T. Plasma Sci.* **26** No 3, 366 (1998).
- N.S. Ginsburg, I.V. Zotova, A.S. Sergeev, V.Y. Zaslavsky, I.V. Zheleznov, *Phys. Rev. Lett.* **108**, 105101 (2012).
- S.A. Kishko, A.N. Kuleshov, S.S. Ponomarenko, B.P. Yefimov, *Vestnik KHNU. Ser. Radiofizika i Elektronika* **21** No 1038, 83 (2012).
- S.A. Kishko, A.N. Kuleshov, B.P. Yefimov, *Vestnik KhNU. Ser. Radiofizika i Elektronika* **23** No 1094, 14 (2013).
- R. Hirose, T. Kamikado, Y. Okui, *IEEE T. Appl. Superconductivity* **18** No 2, 920 (2008).
- M.Yu. Glyavin, K.A. Zhurin, Ye.A. Kopelovich, A.G. Luchinin, M.V. Morozkin, F.A. Flat, *Pribory i tekhnika eksperimenta* **1**, 84 (2011).
- D. Gloge, *Raschet opticheskikh rezonatorov i linzovykh sistem* (Kvazioptika. Moskva: Mir: 1966).
- N.A. Zavolsky, V.E. Zapevalov, M.A. Moiseev, *Radiophys. Quantum Electron.* **49** No 2, 108 (2006).
- Sh.Ye. Tsimring, *Vvedeniye v vysokochastotnyuyu vakuumnyuyu elektroniku i fiziku elektronnykh puchkov* (Nizhniy Novgorod: IPF RAN: 2012).
- S.G. Kalashnikov, *Elektrichestvo* (Moskva: Nauka: 1977).
- S.A. Kishko, A.N. Kuleshov, M.Yu. Glyavin, I.V. Zotova, I.V. Zheleznov, N.S. Ginzburg, V.N. Manuilov, V.Yu. Zaslavskii, *J. Commun. Technol. Electron.* **59** No 7, 777 (2014).